

A New Deformable Model Using Dynamic Gradient Vector Flow and Adaptive Balloon Forces

Suhuai Luo, Rongxin Li, and Sébastien Ourselin
CSIRO Telecommunications & Industrial Physics
Medical Imaging Group
Cnr Vimiera & Pembroke Rd, Marsfield NSW 2122, Australia
suhuai.luo@csiro.au

Abstract

An extension of the gradient vector flow snake (GVF snake) is presented. The method is based on combining two other external forces. First, the adaptive balloon force has been developed to increase the GVF snake's capture range and convergence speed. Then, a dynamic GVF force is introduced to provide an efficient evolution-stop mechanism. In this way, we prevent the snake from breaking through the correct surface and locking to other salient feature points. Preliminary segmentation results demonstrate the potential of our approach in comparison with the original GVF snake method.

1. Introduction

There has been a substantial amount of research on segmenting images with deformable models in recent years [4]. Notably active contours, known as “snakes”, have been widely studied and applied in medical image analysis, their applications including edge detection, segmentation of objects, shape modeling and motion tracking [7, 11]. Snakes were first introduced in 1987 by Kass *et al.* [5]. They generally represent an object boundary as a parameter curve or surface. An energy function is associated with the curve, so the problem of finding an object boundary is cast as an energy minimisation process. Typically, the curves are affected by both an internal force and external force. A snake can locate object contours well, once an appropriate initialisation is done. However, since the energy minimisation is carried out locally, the located contours can be trapped by a local minimum. A number of methods have been proposed to improve the snake's performance [8, 1]. A balloon model was introduced by Cohen *et al.* to enlarge the snake's capture range [2, 3]. Recently, Xu *et al.* have proposed a new deformable model called the “gradient vector flow

snake” (GVF) [11, 12]. Instead of directly using image gradients as an external force, it uses a spatial diffusion of the gradient of an edge map of the image. GVF snake was proposed to address the traditional snake's problems of short capture range and inability to track at boundary concavity. But GVF still may not be able to capture object contours in some medical image segmentation. Efforts at improving the original GVF snake's performance have been published recently. Xu *et al.* combined GVF force with a constrained balloon force to segment gyri in the cortex [10]. Although this combination works well on this case, its requirement of an *a priori* knowledge of the region of interest may restrict its application. Yu *et al.* proposed to compute the GVF using a polar coordinate representation instead of cartesian coordinates [13]. In this way, the method can perform better than the original GVF snake in areas of long thin boundary concavities and boundary gaps. But the capture range of this improved GVF does not seem larger than the original method.

In our paper, after presenting the properties of the GVF snake, we propose a new approach to enhance the GVF snake performance on segmentation. The method consists of two major parts. First, an adaptive balloon force is incorporated into internal forces to increase capture range and speed-up evolution. Secondly, a dynamic GVF force is introduced to provide an evolution-stop mechanism. With this ability, the located contours are less sensitive to local minima.

This paper is organized as follows. First the mathematic foundation of active contour models, including conventional snakes and GVF snakes, are introduced in section 2. We detail in section 3 the different aspects of our improved GVF snake using an adaptive ballon model and a dynamic GVF. In section 4, we present some preliminary results of tumour segmentation on brain MRI and compare the performance of our approach with the GVF snake. Finally, we propose several avenues of research for future work in

section 5.

2. Active Contour Models

In this section, we review the mathematic formulation of conventional snakes and GVF snakes. We also describe the strengths and weakness of each method.

2.1 Snakes

In 2D, a snake is a curve $\mathbf{C}(s) = (x(s), y(s))$ where $s \in [0, 1]$. The curve moves through the image domain to minimize a specified energy function. In traditional snakes, the energy is usually formed by internal forces and external forces as:

$$E_{snake} = E_{internal} + E_{external} \quad (1)$$

$E_{internal}$ tends to elastically hold the curve together (elasticity forces) and to keep it from bending too much (bending forces). This energy is defined in equation (2), where \mathbf{C}_s and \mathbf{C}_{ss} represent the first and second derivative respectively. We can control the snake's tension and rigidity by the coefficients α and β .

$$E_{internal} = \frac{1}{2} \int_s \alpha |\mathbf{C}_s|^2 ds + \frac{1}{2} \int_s \beta |\mathbf{C}_{ss}|^2 ds \quad (2)$$

$E_{external}$ intends to pull or push the curve towards the edges. Typically, the external forces consist of potential forces. This energy is defined in equation (3), where E_{image} represents the negative gradient of a potential function. This energy is generally the image force as defined in equation (4) where I denotes the image and $\mathbf{x} = \mathbf{x}(x, y) = [x \ y]^t$.

$$E_{external} = \int_s E_{image}(\mathbf{C}(s)) ds \quad (3)$$

$$E_{image}(\mathbf{x}) = -|\nabla I(\mathbf{x})|^2 \quad (4)$$

Using variational calculus and the Euler-Lagrange differential equation, we can solve equation (1). Then, the solution of this force balance, as defined in equation (5), represents the snake final position. The differences in the ways the energy function is established will result in different snakes.

$$\alpha \mathbf{C}_{ss} - \beta \mathbf{C}_{ssss} - \nabla E_{image} = 0 \quad (5)$$

Although the traditional snakes have found many applications, they are intrinsically weak in three main aspects: First, they are very sensitive to parameters. Second they have small capture range and the convergence of the algorithm is mostly dependent of the initial position. Finally,

they have difficulties in progressing into boundary concavities.

2.2 GVF snakes

Xu *et al.* have proposed a new GVF snake to achieve better object segmentation [12]. The basic idea of the GVF snake is to extend influence range of image force to a larger area by generating a GVF field. The GVF field is computed from the image. In detail, a GVF field is defined as a vector field $\mathbf{V} = \mathbf{V}(\mathbf{x})$ that minimizes the energy function

$$Q = \iint \mu \nabla^2 \mathbf{V} + |\nabla f|^2 |\mathbf{V} - \nabla f|^2 d\mathbf{x} \quad (6)$$

where f is the edge map which is derived by using an edge detector on the original image convoluted with a Gaussian kernel, and μ is a regularization parameter. Using variational calculus, the GVF field can be obtained by solving the corresponding Euler-Lagrange equations.

Similar to equation (5), the force balance equation of GVF snake can be expressed as

$$\alpha \mathbf{C}_{ss} - \beta \mathbf{C}_{ssss} + \gamma \mathbf{V} = 0 \quad (7)$$

where γ is a proportional coefficient. GVF snake's larger capture range and concavity tracking ability are attributed to the diffusion operation shown in the above equation. When $|\nabla f|$ is small, the energy is dominated by the sum of the squares of the partial derivatives of the vector field, resulting a slowly varying yet large coverage field. Whereas when $|\nabla f|$ is large, the second term dominates the integral.

In applying the GVF snake on real data such as medical images, the capture range of the active contour did not seem as large as we expected. This is mainly because in the case of medical data, images often contain a lot of textures. Unfortunately, the GVF field is very sensitive to these variations and the active contour does not converge to the ideal solution. Another observation was that the GVF snake was sensitive to the shape irregularities. In these cases, the GVF force could not properly push the snake to the right contour.

To deal with these problems we have developed an improved GVF snake. This new method is presented in detail in the following section.

3 Improved GVF snake

The improvement we propose is to add new external forces, including an adaptive balloon force f_{pa} and a dynamic GVF force, defined as a vector field \mathbf{V}_{dyn} . Then, we propose a new scheme to integrate these external forces in the snake mathematic formulation.

3.1 Adaptive balloon force

In the balloon model proposed by Cohen *et al.*, a pressure force $f_p(s)$ is added to snake force as a second external force to push the curve outward or inward [2, 3]. In this way, the curve is considered as a balloon that has been inflated or deflated. Equation (8) represents the pressure force, where $\vec{n}(s)$ is the normal unit vector to the curve at point $\mathbf{C}(s)$.

$$f_p(s) = k \cdot \vec{n}(s) \quad (8)$$

The balloon force is considered to increase the image potential force capture range. This is a proper consideration given that the snake can be set to start evolving inside the object. Unfortunately, balloon force introduces unpredictability to the performance of the active contour and make it more sensitive to the value of its different parameters.

To overcome the unpredictability problem introduced by the balloon force, this force is applied in an adaptive way. The main idea is to give the balloon force bigger weight compared to the GVF force at the early stage of the evolution, and to give the balloon force smaller weight at the later stage. In this way, the speed of the convergence is increased, and the snake can be correctly pushed toward the surface even if it starts far away with less chance of being over-pushed.

3.2 Dynamic GVF force

A dynamic GVF force is introduced to provide a unique evolution-stop mechanism as well as all the characteristics owned by the original GVF force. The evolution-stop mechanism is needed to prevent the snake from breaking through the correct contour and locking to other feature points. The breakage can happen in areas where two objects or organs are very close each other. The introduction of the dynamic GVF force is inspired by a property of the GVF field. That is, when the GVF field passes a contour, its direction will change. Figure 1 shows an ellipse and its corresponding gradient vector flow.

It can be easily observed that the field vector changes direction at the ellipse boundary. Therefore, a consistency degree is incorporated into the new dynamic GVF force. The force varies according to the consistency. If the evolution of the snake will cause the change of GVF force direction, it is said inconsistency has occurred and the snake is not allowed to evolve to the new position.

3.3 New scheme

With these two novel inclusions, the proposed force balance equation can be expressed as:

$$\alpha \mathbf{C}_{ss} - \beta \mathbf{C}_{ssss} + \gamma \mathbf{V}_{dyn} + \lambda f_{pa} = 0 \quad (9)$$

\mathbf{V}_{dyn} is defined in equation (10) as a dynamic gradient vector flow force. Let \mathbf{x}_1 be a point on the current snake and \mathbf{x}_2 its possible next position in the evolution process. C_θ defines the consistency angle and is proportional to the angle between the GVF vectors at \mathbf{x}_1 and \mathbf{x}_2 . T_θ represents the cut-off angle: based in our experiments, $T_\theta = 20^\circ$ is a good threshold.

$$\mathbf{V}_{dyn} = \begin{cases} \mathbf{V} & \text{if } C_\theta > T_\theta \\ \frac{-\alpha \mathbf{C}_{ss} + \beta \mathbf{C}_{ssss} - \lambda f_{pa}}{\gamma} & \text{otherwise} \end{cases} \quad (10)$$

The new dynamic gradient vector flow force will be the same as conventional GVF if the snake point moves towards the contour. But when the snake point tries to cross over an edge, the dynamic gradient vector flow force will stop the point from moving. The threshold T_θ will decide when this evolution-stop mechanism will be triggered.

4 Experiments

Brain Tumor Segmentation Database. In validating the performance of the proposed method, we used the SPL and NSG Brain Tumor Segmentation Database [6, 9]. The database consists of magnetic resonance images of several anonymous brain tumor patients, as well as segmentations of the brain and tumor from these scans (MR T1-weighted image in the sagittal plane, $256 \times 256 \times 124$, $0.9375 \times 0.9375 \times 1.5 \text{ mm}^3$). Manual segmentations obtained by neurosurgeons and automated segmentations obtained by the method of [6] and [9]. In figure 3, we present the manual segmentation of a *glioma* on the MRI of the patient 4 in the database, the slice 35 is presented.

Validation criteria. Our validation criteria of tumor segmentation is based on both subjective and quantitative analysis. For subjective aspect, the contours drawn by experts (figure 3) and by automatic segmentation were compared (figure 4). For quantitative analysis, three validating parameters are defined. In defining the parameters, the accuracy of the snake results is checked against the manual segmentations done by four experts.

To evaluate the results, we propose to use three values which we will denote by C_r , FPN and FNN .

C_r is defined as the ratio between the area considered as tumor by both the snake and at least three experts and the area considered as tumor either by the snake or at least three experts. It is expressed as $C_r = \frac{A_\cap}{\max(A_{expert}, A_s)}$, where A_s is the area confined by snake; A_{expert} is the area considered as tumor by at least three of the four experts and A_\cap is the

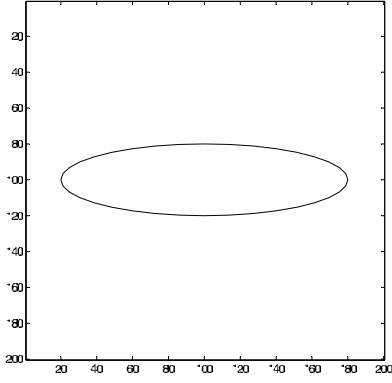


Figure 1. An ellipse and its corresponding GVF forces.

area overlapped between A_s and A_{expt} . We can note that C_r is a normalized value ($C_r \in [0, 1]$).

FPN is defined as the area considered as tumor by snake, but as non-tumor by at least 3 experts (False Positive Number).

FNN is defined as the area considered as non-tumor by snake, but as tumor by at least 3 experts (False Negative Number).

Results. To investigate the performance of our segmentation method and compare it with original GVF snake, we have designed four experiments using four different sets of parameters. For each experiment, both original GVF snake and our improved GVF snake have the same values of α , β and γ , we also the initial position for the curve. Figure 2 shows the original image and the initial snake position drawn in white curve.

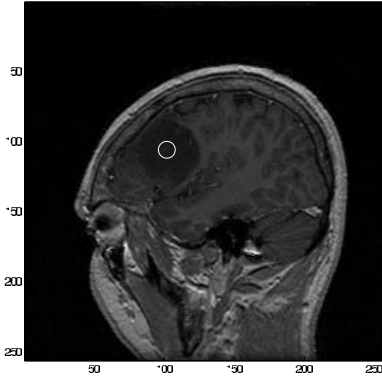
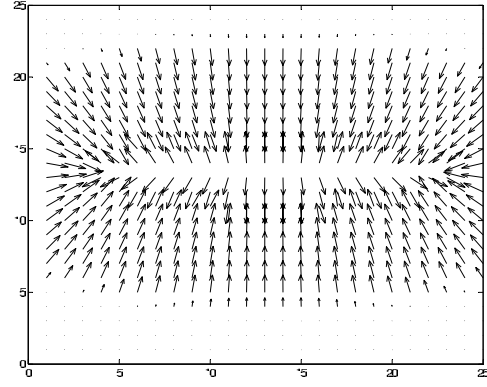


Figure 2. The original MRI slice 35 of patient 4 and the initial snake position drawn in white.

Table 1 summarizes the parameters set for the four experiments, we choose $\lambda = 0.2$ for our method. Table 2



parameters	α	β	γ
Test 1	0.05	0.1	0.3
Test 2	0.05	0.1	0.5
Test 3	0.05	0.1	0.1
Test 4	0.1	0.2	0.3

Table 1. Parameters set for the four experiments.

and 3 presents the values of C_r , FPN and FNN of both the original GVF snake and our improved GVF snake.

Analysis. Based on the figures and tables, two main points can be drawn as to the performance comparison. One point is that in terms of subjective criteria the original GVF snake's capture range is far from enough to locate the tumor and it easily became stuck on unwanted features and failed on most of the cases, whereas the proposed approach succeed in locating the *glioma* in most cases. The other point is that, according to quantitative analysis, our approach resulted more preferable results than the original GVF snake in most cases. One point we want to note is that in some particular cases the original GVF snake presented some better validating values, however, by analysis all the validating values for each case we can state that our method is still more preferable.

Based on figure 4, we can see that the original GVF can not correctly locate the *glioma* and is stuck at the top part of the tumor. For quantitative analysis, by observing the C_r values of the original GVF snake and our approach, we can see that the original GVF snake gives favorable value of 0.8127 comparing to 0.7783 of our approach. This does mean that in this case the area located by the original GVF snake is more likely as *glioma* than the area located by our approach. However, if we check the FPN and FNN values, we can see that our method presented much less false

Original GVF	Test 1	Test 2	Test 3	Test 4
C_r	0.7931	0.8127	0.1388	0.2055
FPN	129	235	0	37
FNN	307	278	1278	1179

Table 2. Values of the three criteria using the original GVF snake.

Improved GVF	Test 1	Test 2	Test 3	Test 4
C_r	0.8455	0.7783	0.6274	0.7871
FPN	259	407	2	389
FNN	67	55	553	46

Table 3. Values of the three criteria using the improved GVF snake.

negative number. This is ideal from the viewpoint of a neurosurgeon.

5 Conclusion

In this paper, we have presented a new method using Gradient Vector Flow and Balloons. We introduced an adaptive balloon force to increase GVF snake's capture range and speed up evolution. Then we proposed a dynamic GVF force to provide an efficient evolution-stop mechanism.

Based on experiments on segmenting a tumor in real brain MRI data, it has shown that the proposed method is robust to the variation in initial position and efficient in preventing the snake from breaking through correct contour and locking to other feature points.

A current limitation of the method is that GVF is computed independently slice by slice (2D version). As a consequence, we do not take into account the interslice spatial continuity of the gradient, or the possible anisotropy of the voxels. Such error of segmentation might be reduced by putting spatial constraints to the reconstructed structure.

Acknowledgments

The authors would like to thank Drs. Simon Warfield, Michael Kaus, Ron Kikinis, Peter Black and Ferenc Jolesz for sharing the tumor database.

References

[1] P. Bamford and B. Lovell. Unsupervised cell nucleus segmentation with active contours. *Signal Processing Special Issue: Deformable Models and Techniques for Image and Signal Processing*, 71(2):203–213, 1998.

[2] L. Cohen. On active contour models and balloons. *Computer Vision, Graphics, and Image Processing: Image Understanding*, 53(2):211–218, 1989.

[3] L. Cohen and I. Cohen. Finite-element methods for active contour models and balloons for 2-d and 3-d images. *IEEE Transactions on Pattern Analysis and Machine Intelligence*, 15(11):1146–1131, November 1993.

[4] A. Jain, Y. Zhong, and M. Dubuisson-Jolly. Deformable template models: A review. *Signal Processing*, 71:109–129, 1998.

[5] M. Kass, M. Witkin, and D. Terzopoulos. Snakes: active contour models. *International Journal of Vision*, 1:321–331, 1987.

[6] M. Kaus, S. Warfield, A. Nabavi, P. Black, F. Jolesz, and R. Kikinis. Automated segmentation of mri of brain tumors. *Radiology*, 218:586–591, 2001.

[7] T. McInerney and D. Terzopoulos. A Dynamic Finite Element Surface Model for Segmentation and Tracking in Multidimensional Medical Images with Applications to Cardiac 4D Image analysis. *Computerized Medical Imaging and Graphics*, 19(1):69–83, 1995.

[8] T. McInerney and D. Terzopoulos. Deformable models in medical image analysis: A survey. *Medical Image Analysis*, 1(2):91–108, 1996.

[9] M. Warfield, S.M. Kaus, F. Jolesz, and R. Kikinis. Adaptive, template moderated, spatially varying statistical classification. *Medical Image Analysis*, 4(1):43–55, 2000.

[10] C. Xu, D. Pham, M. Rettmann, D. Yu, and J. Prince. Reconstruction of the human cerebral cortex from magnetic resonance images. *IEEE Transactions on Medical Imaging*, 18(6):467–479, June 1999.

[11] C. Xu and J. Prince. Generalized gradient vector flow external forces for active contours. *Signal Processing*, 71:131–139, 1998.

[12] C. Xu and J. Prince. Snakes, shapes, and gradient vector flow. *IEEE Transactions on Images Processing*, 7(3):359–369, 1998.

[13] Z. Yu and C. Bajaj. Image Segmentation Using Gradient Vector Diffusion and Region Merging. In *ICPR'02*, pages 828–831, Quebec City, August 11-15 2001.

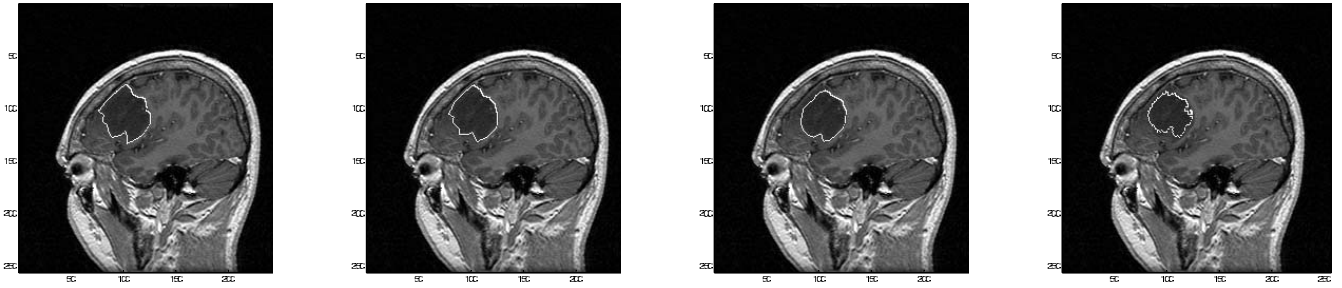


Figure 3. *Manual segmentation by four different experts of a glioma on the MRI.*

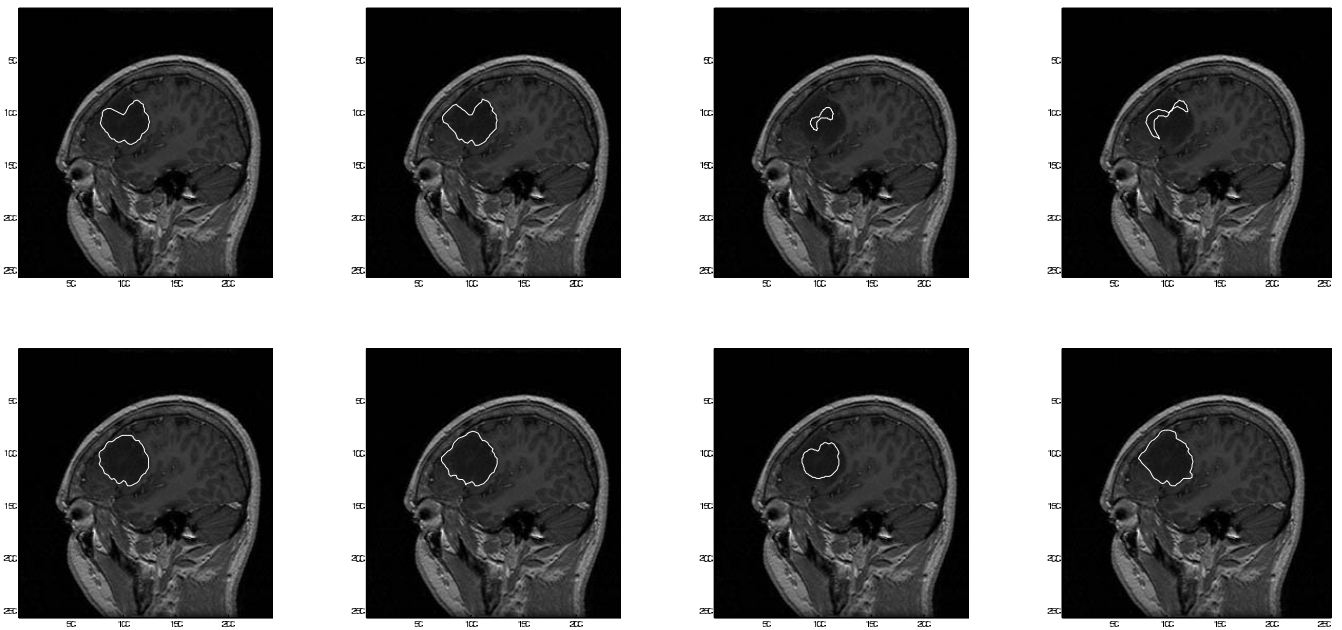


Figure 4. *Automatic Segmentation of the glioma, using two different techniques with four sets of parameters; Top: original GVF snake; Bottom: our improved GVF snake.*